Hyperbolic Harmonic Brain Surface Registration with Curvature-based Landmark Matching

Rui Shi[1], Wei Zeng[2], Zhengyu Su[1], Yalin Wang[3], Hanna Damasio[4], Zhonglin Lu[5], Shing-Tung Yau[6], and Xianfeng Gu[1]

[1] Department of Computer Science@Stony Brook University
[2] School of Computing & Information Sciences@Florida International University
[3] School of Computing, Informatics, and Decision Systems Engineering@Arizona State University
[4] Neuroscience@University of Southern California
[5] Department of Psychology@Ohio State University
[6] Mathematics Department@Harvard University
{rshi@cs.stonybrook.edu;wzeng@cis.fiu.edu;suzy.bryant@gmail.com; Yalin.Wang@asu.edu;hdamasio@college.usc.edu;lu.535@osu.edu;yau@math.harvard.edu;gu@cs.stonybrook.edu}

Abstract. Brain Cortical surface registration is required for inter-subject studies of functional and anatomical data. Harmonic mapping has been applied for brain mapping, due to its existence, uniqueness, regularity and numerical stability. In order to improve the registration accuracy, sculcal landmarks are usually used as constraints for brain registration. Unfortunately, constrained harmonic mappings may not be diffeomorphic and produces invalid registration. This work conquers this problem by changing the Riemannian metric on the target cortical surface to a hyperbolic metric, so that the harmonic mapping is guaranteed to be a diffeomorphism. With landmarks delineated as boundary condition, it is possible to be integrated with landmark matching. The computational algorithms are based on the Ricci flow method and hyperbolic heat diffusion. Experimental results demonstrate that, by changing the Riemannian metric, the registrations have higher qualities in terms of landmark alignment, curvature matching, area distortion and overlapping of region of interests.

1 Introduction

Morphometric and functional studies of human brain require that neuro-anatomical data from a population to be normalized to a standard template. The purpose of any registration methods is to find a map that assigns a correspondence from every point in a subject brain to a corresponding point in the template brain. Due to the anatomical fact, the mapping is required to be smooth and bijective, namely, diffeomorphic. Since cytoarchitectural and functional parcellation of the cortex is intimately related the folding of the cortex, it is important to ensure the alignment of the major anatomic features, such as sucal landmarks.

Harmonic mapping has been commonly applied for brain cortical surface registration. Physically, a harmonic mapping minimizes the "stretching energy", and produces

smooth registration. The harmonic mappings between two hemsiphere cortical surfaces, which were modeled as genus zero closed surfaces, are guaranteed to be diffeomorphic, and angle-preserving [6]. Furthermore, all such kind of harmonic mappings differ by the Möbius transformation group. Numerically, finding a harmonic mapping is equivalent to solve an elliptic partial differential equation, which is stable in the computation and robust to the input noises.

Unfortunately, harmonic mappings with constraints may not be diffeomorphic any more, and produces invalid registrations with flips. In order to overcome this shortcoming, in this work we propose a novel brain registration method, which is based on hyperbolic harmonic mapping. Conventional registration methods map the template brain surface to the sphere or planar domain [6, 7], then compute harmonic mappings from the source brain to the sphere or planar domain. When the target domains are with complicated topologies, or the landmarks, the harmonic mappings may not be diffeomrophic. In contrast, in our work, we slice the brain surfaces along the landmarks, and assign a unique hyperbolic metric on the template brain, such that all the boundaries become geodesics, harmonic mappings are established and guaranteed to be diffeomorphic.

In addition to the guaranteed diffeomorphism, we also addressed a curvature based landmark align method to obtain a geometric meaningful registration. i.e. it maps similarly shaped segments of sulcal curves to each other. We sample the landmark curves and record their curvature information, then use a Dynamic Time Warping algorithm (DTW) to align them together. This step achieves a geometric meaningful registration for landmarks compare to naive arc length interpolation.

In summary, the main contributions of the current work are as follows: First, introduce a novel brain registration method based on hyperbolic harmonic maps, the registration preserves all the merits of conventional harmonic brain registration methods, such as existence, uniqueness, regularity, numerical stability and so on. Second, develop a novel algorithm for computing harmonic mappings on hyperbolic metric using nonlinear heat diffusion method and Ricci flow. Third, develop a curvature based landmark matching method to achieve a geometric meaningful landmark registration. The paper is organized as follows: this section focuses on the motivation and introduction; next section briefly reviews the most related works; section 3 gives theoretic background for hyperbolic harmonic mapping; section 4 details the computational algorithms; section 5 reports our experimental results; section 6 summarizes the current work and points out future research directions.

2 Previous Works

In computer vision and medical imaging research, surface conformal parameterization with the Euclidean metric have been extensively studied [1, 26, 23]. Wang et al. [21] studied brain morphology with Teichmüller space coordinates where the hyperbolic conformal mapping was computed with the Yamabe flow method. Zeng [26] proposed a general surface registration method via the Klein model in the hyperbolic geometry where they used the inversive distance curvature flow method to compute the hyperbolic conformal mapping.

Various non-linear brain volume-based registration models [15, 24] have been developed. However, early research [5, 18] has demonstrated that surface-based approaches may offer advantages as a method to register brain images. To register brain surfaces, a common approach is to compute a range of intermediate mappings to some canonical parameter space [2, 25]. A flow, computed in the parameter space of the two surfaces, then induces a correspondence field in 3D [7, 17]. This flow can be constrained using anatomical landmark points or curves [8, 10], by sub-regions of interest [13], by using currents to represent anatomical variation [3, 20], or by metamorphoses [19]. There are also various ways to optimize surface registrations [12, 16]. Overall, finding diffeomorphic mappings between brain surfaces is an important but difficult problem. In most cases, extra regulations, such as inverse consistency [9, 16], have to be enforced to ensure a diffeomorphism. Since the proposed work offers a harmonic map based scheme for diffeomorphisms which guarantees a perfect landmark curve registration via enforced boundary matching, the novelty of the proposed work is that it facilitates diffeomorphic mapping between general surfaces with delineated landmark curves.

3 Theoretic Background

This section briefly introduces the theoretic foundations for the current work. We refer readers to [14] for more thorough exposition of harmonic maps, [26] for Ricci flow.

Hyperbolic Harmonic Map Suppose S is an oriented surface with a Riemannian metric $\mathbf{g}$. One can choose a special local coordinates (x, y), the so-called *isothermal parameters*, such that $\mathbf{g} = \sigma(x, y)(dx^2 + dy^2) = \sigma(z)dzd\bar{z}$, where the complex parameter $z = x + iy$, $dz = dx + idy$. An atlas consisting of isothermal parameter charts is called an *conformal structure*. The *Gauss curvature* is given by $K(z) = -\frac{2}{\sigma(z)}\frac{\partial^2}{\partial z \partial \bar{z}} \log \sigma(z)$, where the complex differential operator $\frac{\partial}{\partial z} = \frac{1}{2}(\frac{\partial}{\partial x} + i\frac{\partial}{\partial y})$, $\frac{\partial}{\partial \bar{z}} = \frac{1}{2}(\frac{\partial}{\partial x} - i\frac{\partial}{\partial y})$. If $K(z)$ is -1 everywhere, then we say the Riemannian metric is *hyperbolic*. The Gauss-Bonnet theorem claims that the total Gauss curvature is a topological invariant $\int_S K(p)dp = 2\pi\chi(S)$, where $\chi(S)$ is the Euler-characteristic number. Given a mapping $f : (S_1, \mathbf{g}_1) \to (S_2, \mathbf{g}_2)$, z and w are local isothermal parameters on S_1 and S_2 respectively. $\mathbf{g}_1 = \sigma(z)dzd\bar{z}$ and $\mathbf{g}_2 = \rho(w)dwd\bar{w}$. Then the mapping has local representation $w = f(z)$ or denoted as $w(z)$.

Definition 1 (Harmonic Map). *The* harmonic energy *of the mapping is defined as* $E(f) = \int_S \rho(z)(|w_z|^2 + |w_{\bar{z}}|^2)dxdy$. *If f is a critical point of the harmonic energy, then f is called a* harmonic map.

The necessary condition for f to be a harmonic map is the Euler-Lagrange equation $w_{z\bar{z}} + \frac{\rho_w}{\rho} w_z w_{\bar{z}} \equiv 0$. The theory on the existence, uniqueness and regularity of harmonic maps have been thoroughly discussed in [14]. The following theorem lays down the theoretic foundation of our proposed method.

Theorem 1. [14] *Suppose $f : (S_1, \mathbf{g}_1) \to (S_2, \mathbf{g}_2)$ is a degree one harmonic map, furthermore the Riemann metric on S_2 induces negative Gauss curvature, then for each homotopy class, the harmonic map is unique and diffeomorphic.*

Ricci Flow Ricci flow deforms the Riemannian metric proportional to the curvature, such that the curvature evolves according to a heat diffusion process and eventually becomes constant everywhere.

Definition 2 (Ricci Flow). *Hamilton's surface Ricci flow is defined as* $\frac{dg_{ij}}{dt} = -2Kg_{ij}$.

Theorem 2 (Hamilton). *Let* $(S, \mathbf{g})$ *be compact. If* $\chi(S) < 0$*, then the solution to Ricci Flow equation exists for all* $t > 0$ *and converges to a metric of constant curvature.*

Given a surface with negative Euler-characteristic number, by running Ricci flow, a hyperbolic metric of the surface can be obtained. Then for each point $p \in S$, we can choose a neighborhood U_p and isometrically embed it onto the hyperbolic plane $\mathbb{H}^2$, $\phi_p : U_p \to \mathbb{H}^2$. (U_p, ϕ_p) is an isothermal coordinate chart, the collection of such charts $\{(U_p, \phi_p)|\forall p \in S\}$ forms a conformal structure of the surface.

Hyperbolic Space In this work, we use the Poincaré's disk model for the hyperbolic plane $\mathbb{H}^2$, $\{z \in \mathbb{C}| \ |z| < 1\}$ with Riemannian metric $\rho(z)dzd\bar{z} = \frac{dzd\bar{z}}{(1-z\bar{z})^2}$. The geodesics are called *hyperbolic lines*. A hyperbolic line through two points p and q is a circular arc perpendicular to the unit circle. The hyperbolic rigid motions are Möbius transformations $\phi : z \to e^{i\theta}\frac{z-z_0}{1-\bar{z_0}z}$. A *fixed point* p of a Möbius transformation ϕ satisfies $\phi(z) = z$. All the Möbius transformations in the current work have two fixed points z_1 and z_2, $z_1 = \lim_{n\to\infty}\phi^n(z), z_2 = \lim_{n\to\infty}\phi^{-n}(z)$, The *axis* of ϕ is the hyperbolic line through its fixed points. Given two non-intersecting hyperbolic lines γ_1 and γ_2, there exists a unique hyperbolic line τ orthogonal to both of them, and gives the shortest path connecting them. For each γ_k, there is a unique reflection ϕ_k whose axis is γ_k, then the axis of $\phi_2 \circ \phi_1^{-1}$ is τ. Another hyperbolic plane model is the Klein's disk model, where the hyperbolic lines coincide with Euclidean lines. The conversion from Poincare's disk model to Klein disk model is given by $z \to \frac{2z}{1+z\bar{z}}$.

Fundamental Group and Fuchs Group Let S be a surface, all the homotopy classes of loops form the fundamental group (homotopy group), denoted as $\pi_1(S)$. A surface $\tilde{S}$ with a projection map $p : \tilde{S} \to S$ is called the *universal covering space* of S. The Deck transformation $\phi : \tilde{S} \to \tilde{S}$ satisfies $\phi \circ p = p$ and form a group $Deck(\tilde{S})$. Let γ be a loop on the hyperbolic surface, then its homotopy class $[\gamma]$ corresponds to a unique Möbius transformation ϕ_γ. As the Gauss curvature of S is negative, in each homotopy class $[\gamma]$, there is a unique geodesic loop given by the axis of ϕ_γ.

Hyperbolic Pants Decomposition As shown in Fig.2 (a) and (b), given a topological surface S, it can be decomposed to pairs of pants. Each pair of pants is a genus zero surface with three boundaries. If the surface is with a hyperbolic metric, then each homotopy class has a unique geodesic loop. Suppose a pair of hyperbolic pants with three boundaries $\{\gamma_i, \gamma_j, \gamma_k\}$, which are geodesics. Let $\{\tau_i, \tau_j, \tau_k\}$ be the shortest geodesic paths connecting each pair of boundaries. The shortest paths divide the surface to two identical hyperbolic hexagons with right inner angles. When the hyperbolic hexagon with right inner angles is isometrically embedded on the Klein disk model, it is identical to a convex Euclidean hexagon.

4 Algorithms

We first explain our registration algorithm pipeline as illustrated in Alg. 1 and Fig. 1, then explain each step in details as following:

Algorithm 1 Brain Surface Registration Algorithm Pipeline.

1. Slice the cortical surface along the landmark curves.
2. Compute the hyperbolic metric using Ricci flow.
3. Hyperbolic pants decomposition, isometrically embed them to Klein model.
4. Compute harmonic maps using Euclidean metrics between corresponding pairs of pants, with consistent curvature based boundary matching constraints computed by the DWT algorithm.
5. Use nonlinear heat diffusion to improve the mapping to a global harmonic map on Poincare disk model.

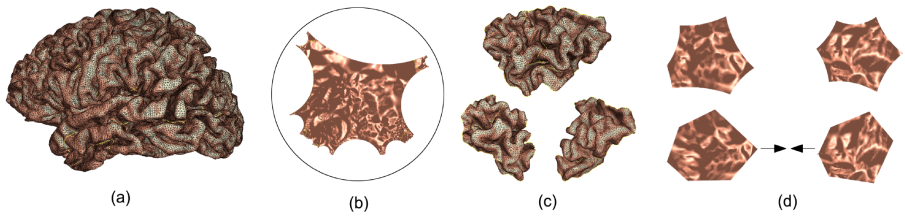

Fig. 1. Algorithm Pipeline (suppose we have 2 brain surface M and N as input): (a). One of the input brain models M, with landmarks being cut open as boundaries. (b). Hyperbolic embedding of the M on the Poincaré disk. (c). Decompose M into multiple pants by cuting the landmarks into boundaries, and each pant is further decomposed to 2 hyperbolic hexagons. (d). Hyperbolic hexagons on Poincaré disk become convex hexagons under the Klein model, then a one-to-one map between the correspondent parts of M and N can be obtained. Then we can apply our hyperbolic heat diffusion algorithm to get a global harmonic diffeomorphism.

1. Preprocessing The cortical surfaces are reconstructed from MRI images and represented as triangular meshes. The sucul landmarks are manually labeled on the edges of the meshes. Then we slice the meshes along the landmark curves, to form topological multiple connected annuli.

2. Discrete Hyperbolic Ricci Flow As the Euler characteristic numbers of the cortical surfaces are negative, they admit hyperbolic metrics. We treat each triangle as hyperbolic triangle and set the target Gauss curvature for each interior vertex to be zeros, and the target geodesic curvature for each boundary vertex to be zeros as well. We compute the hyperbolic metrics of the brain meshes using discrete hyperbolic Ricci flow method. For detailed discussion of the computational algorithm, one may refer to [26].

3. Hyperbolic Pants Decomposition In our work, the input surface is a genus zero surface with multiple boundary components $\partial S = \gamma_0 + \gamma_1 + \cdots \gamma_n$, moreover, the surface is with hyperbolic metric, and all boundaries are geodesics. The algorithm is as follows: choose arbitrary two boundary loops γ_i and γ_j, compute their product $[\gamma_i \cdot \gamma_j]$, if the product is homotopic to $[\gamma_k^{-1}]$, then choose other pair of boundary loops. Otherwise, suppose $[\gamma_i \cdot \gamma_k]$ is not homotopic to any boundary loop, compute its corresponding Möbius transformation, $\phi_{\gamma_i\gamma_j}$, and its fixed points $\phi^{+\infty}_{\gamma_i\gamma_j}(0)$ and $\phi^{-\infty}_{\gamma_i\gamma_j}(0)$. The hyperbolic line through the fixed points is the axis of the $\phi_{\gamma_i\gamma_j}$, which is the geodesic in $[\gamma_i\gamma_j]$. Slice the mesh along the geodesic, and repeat the process on each connected components, until all the connected components are pairs of pants. Figure 2 (c),(d) shows one example for the decomposition process. Alg. 2 gives the computational steps.

Algorithm 2 Hyperbolic Pants Decomposition.

Input: Topological sphere M with B boundaries.
Output: Pants decomposition of M.
1. Put all boundaries γ_i of M into a queue Q.
2. If Q has < 3 boundaries, end; else goto Step 2.
3. Compute a geodesic loop γ' homotopic to $\gamma_i \cdot \gamma_j$
4. γ', γ_i and γ_j bound a pants patch, remove this pants patch from M. Remove γ_i and γ_j from Q. Put γ' into Q. Go to Step 1.

4. Initial Mapping Constructing with Dynamic Time Warping This step has several stages: first the pants are decomposed to hyperbolic hexagons and embed isometrically to the Poincaré disk; then convert the hexagons from Poincaré disk to Klein model; the final, also the most important step is to register the corresponding hexagons using Dynamic Time Warping (DTW) to achieve a geometric meaningful landmark matching and harmonic mapping for surface registration. The resultant piecewise harmonic mapping is the initial mapping. Fig 2 (e) shows the algorithm process.

For the first stage, we use the method described in the theory section to find the shortest path between two boundary loops. Assume a pair of hyperbolic pants M with three geodesic boundaries $\{\gamma_i, \gamma_j, \gamma_k\}$. On the universal covering space $\tilde{M}$, γ_i and γ_j are lifted to hyperbolic lines, $\tilde{\gamma}_i$ and $\tilde{\gamma}_j$ respectively. There are reflections $\tilde{\phi}_i$ and $\tilde{\phi}_j$, whose symmetry axis are $\tilde{\gamma}_i$ and $\tilde{\gamma}_j$. Then the axis of the Möbius transformation $\tilde{\gamma}_j \cdot \tilde{\gamma}_i^{-1}$ corresponds to the shortest geodesic path τ_k between γ_i and γ_j. In the second stage, each hyperbolic hexagon on the Poincaré disk is transformed to a convex hexagon in Klein's disk using $z \to \frac{2z}{1+z\bar{z}}$. The final step first register the correspondent landmarks, which are the boundaries of hyperbolic hexagon now, using DTW algorithm, then a planar harmonic map between two corresponding planar hexagons is established by $w_{z\bar{z}} \equiv 0$.

DTW algorithm [4] has being proved to be extremely efficient for detecting similar shapes with different phases. Given two curves $X = (x_1; x_2; ...x_N)$ and $Y = (y_1; y_2; ...y_M)$ represented by the sequences of vertices, DTW yields optimal matching solution in the $O(MN)$ time. Here the local cost function is defined as $c_{ij} =$

$|MeanCurvature(x_i) - MeanCurvature(y_j)|$, and the global cost function is $C_{XY} = \sum_{l=1}^{L} c(x_{n_l}, y_{m_l})$. with L be the alignment path length. The result will align two curves according to their mean curvature distribution, which captures the geometry information. One thing worth mentioning is that to ensure the mapping between 2 curves is diffeomorphic, we locally turbulent the result if two vertices i and $i+1$ were mapped to one vertex j. For more detail about DTW algorithm we refer readers to [4].

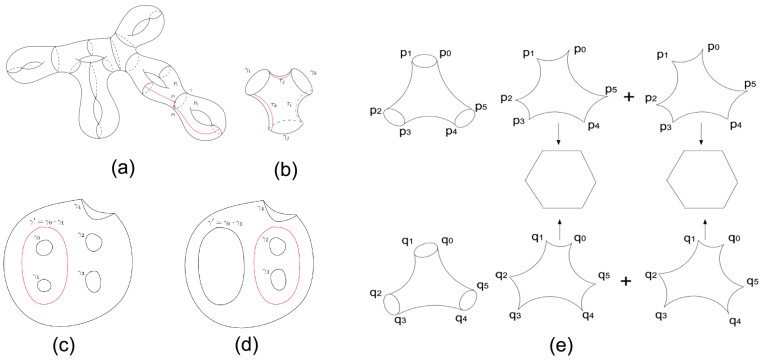

Fig. 2.

5. Non-linear Heat Diffusion Let $(S, \mathbf{g})$ be a triangle mesh with hyperbolic metric $\mathbf{g}$. Then for each vertex $v \in S$, the one ring neighboring faces form a neighborhood U_v, the union of U_v's cover the whole mesh, $S \subset \bigcup_{v \in S} U_v$. Isometrically embed U_v to the Poincaré's disk $\phi_v : U_v \to \mathbb{H}^2$, then $\{(U_v, \phi_v)\}$ form a conformal atlas. All the following computations are carried out on local charts of the conformal atlas. The computational result is independent of the choice of local parameters.

The initial mapping is diffused to form the hyperbolic harmonic map. Suppose $f : (S_1, \mathbf{g}_1) \to (S_2, \mathbf{g}_2)$ is the initial map, $\mathbf{g}_1$ and $\mathbf{g}_2$ are hyperbolic metrics. We compute the conformal atlases of S_1 and S_2, then choose local conformal parameters z and w for S_1 and S_2. The mapping f has local representation $f(z) = w$, or simply $w(z)$, then the non-linear diffusion is given by

$$\frac{dw(z,t)}{dt} = -[w_{z\bar{z}} + \frac{\rho_w(w)}{\rho(w)} w_z w_{\bar{z}}], \tag{1}$$

where $\rho(w) = (1 - w\bar{w})^{-2}$. Suppose v_i is chosen to be a vertex on S_1, with local representation z_i, after diffusion, we get the local representation of its image $w(z_i)$. Suppose $w(z_i)$ is inside a triangular face $t(v_i)$ of S_2, $t(v_i)$ has three vertices with local representation $[w_i, w_j, w_k]$, then we compute the *complex cross ratio*, which is given by $\eta(v_i) := [w(z_i), w_i, w_j, w_k] = \frac{(w(z_i)-w_i)(w_j-w_k)}{(w(z_i)-w_k)(w_j-w_i)}$. the image of v_i is then represented by the pair $[t(v_i), \eta(v_i)]$. Note that, all the local coordinates transitions in the conformal chart of S_1 and S_2 are Möbius transformations, and the cross ration η is

Algorithm 3 Hyperbolic Heat Diffusion Algorithm.

Input: Two surface models M, N with their hyperbolic metric C_M and C_N on Poincaré disk, the one-to-one correspondence (v_i, p_i) and a threshold ε. Here v_i is the vertex of mesh M, p_i is the 3D coordinate on mesh N.
Output: A new diffeomorphism (v_i, P_i).
1. For each vertex v_i of M that is not a landmark vertex, embed it's neighborhood onto Poincaré disk, in which v_i has coordinate z_i; do the same for p_i and note it's coordinate on Poincaré disk as w_i.
2. Compute $\frac{dw_i(z_i,t)}{dt}$ using equation (1).
3. Update $w_i = w_i + step\frac{dw_i(z_i,t)}{dt}$.
4. Compute new 3D coordinate P_i on N using the updated w_i, and repeat the above process until $\frac{w_i(z_i,t)}{dt}$ is less than ε.

invariant under Möbius transformation, therefore, the representation of the mapping $f : v_i \to [f(v_i), \eta(v_i)]$ is independent of the choice of local coordinates. Alg. 3 gives the process by steps. Notice that we may choose to apply the heat diffusion to the landmark vertices in order to get a soft landmark alignment.

5 Experimental Results

We implemented our algorithms using generic C++ on Windows, all the experiments are conducted on a laptop computer of Intel Core2 T6500 2.10GHz with 4GB memory.

Input Data We perform the experiments on 24 brain cortical surfaces reconstructed from MRI images. Each cortical surface has about $150k$ vertices, $300k$ faces and used in some prior research [10]. On each cortical surfaces, a set of 26 landmark curves were manually drawn and validated by neuroanatomists. In our current work, we selected 10 landmark curves, including Central Sulcus, Superior Frontal Sulcus, Inferior Frontal Sulcus, Horizontal Branch of Sylvian Fissure, Cingulate Sulcus, Supraorbital Sulcus, Sup. Temporal with Upper Branch, Inferior Temporal Sulcus, Lateral Occipital Sulcus and the boundary of Unlabeled Subcortcial Region.

Registration Visualization In Fig 3 we show the visualized registration result of 3 brain models, with one as target and 2 registered to it. We can see our algorithm shows a reasonable good result.

Landmark Curve Variation For brain imaging research, it is important to achieve consistent local surface matching, e.g. landmark matching. We adapted a geometric quantitative measure of curve alignment error function to be the global cost function in section 4.4 $C_{XY} = \sum_{l=1}^{L} c(x_{n_l}, y_{m_l})$. For two curves $X = (x_1; x_2; ...x_N)$ and $Y = (y_1; y_2; ...y_M)$ represented by the sequences of vertices. Lower values indicate better geometric alignment for the curves. The DTW algorithm minimizes this error function while keeps the Hausdorff distance to be exactly zero. In Fig. 4 left we show the average histogram of curvature difference of aligned vertices on all 10 landmarks, from both the previous method [7] and our method.

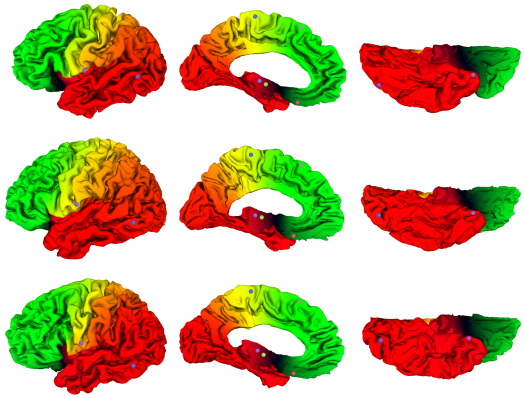

Fig. 3. First row: target brain surface from front, back and bottom view. Rest three rows: 2 brain models registered to the target model. The colored balls on the models show the detailed correspondence, as the balls with the same color are correspondent to each other.

Performance Evaluation and Comparison We compare our registration method with conventional cortical registration method based on harmonic mapping with Euclidean metric [22], where the template surface is conformally flattened to a planar disk, then the registration is obtained by a harmonic map from the source cortical surface to the disk with landmark constraints. Our experimental results show that by replacing Euclidean metric by hyperbolic metric on the source and target cortical surfaces, the quality of the registrations have been improved prominently.

5.1 Diffeomorphism

One of the most important advantages of our registration algorithm is that it ensure the mapping between two surfaces to be diffeomorphic. We randomly choose one model as template and all others as source to compute the registration. For each registration, we compute the Jacobian determinant and measure the areas of flipped regions. The ratio between flipped area to the total area is collected to form the histogram shown in Fig.4 right. The horizontal axis shows the flipped area ratio, the vertical axis shows the number of registrations. The conventional method (blue bars) [22] produces a big flipped area ratio, even as much as 9%. In contrast, the flipped area ratios for all registrations obtained by the current method are exactly 0's.

5.2 Curvature Maps

One method to evaluate registration accuracy is to compare the alignment of curvature maps between the registered models [11]. In this paper we calculated curvature maps using an approximation of mean curvature, which is the convexity measure. We quantified the effects of registration on curvature by computing the difference of curvature maps from the registered models. As Figure 5 left shows, we assign each vertex the

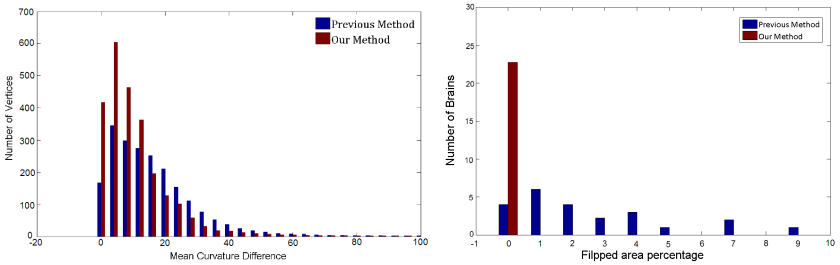

Fig. 4. Left: Landmark curvature difference of previous method and our method. Y axis is the vertex number on landmark that have the X amount of curvature difference. Right: Flipped area percentage of previous method and our method.

curvature difference between its own curvature and the curvature of its correspondent point on the target surface, then build a color map according to the difference.

We use all 24 data sets for the experiment. First, one data set is randomly chosen as the template, then all others are registered to it. For each registration, we compute the curvature difference map. Then we compute the average of 23 curvature difference maps. The average curvature difference map is color encoded on the template, as shown in Fig.5 left. The histogram of the average curvature difference map is also computed, as shown in Fig.5 right. It is obvious that the current registration method produces less curvature errors than [22].

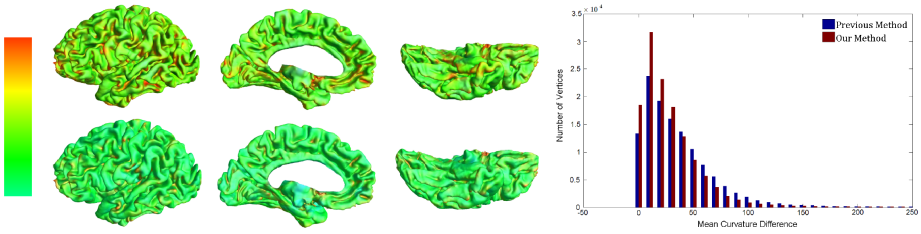

Fig. 5. Left: Curvature map difference of previous method (top row) and our method (bottom row). Color goes from green-yellow-red while the curvature difference increasing. Right: Average Curvature Map Difference of previous method and our method.

5.3 Local Area Distortion

Similarly, we measured the local area distortion induced by the registration. For each point p on the template surface, we compute its Jacobian determinant $J(p)$, and represent the local area distortion function at p as $\max\{J(p), J^{-1}(p)\}$. J can be approximated by the ratio between the areas of a face and its image. Note that, if the registration is not diffeomorphic, the local area distortion may go to ∞. Therefore, we add a

threshold to truncate large distortions. Then we compute the average of all local area distortion functions induced by the 23 registrations on the template surface. The average local area distortion function on the template is color encoded as shown in Fig.6 left, the histogram is also computed in Fig.6 right. It can be easily seen that current registration method greatly reduces the local area distortions compare with [22].

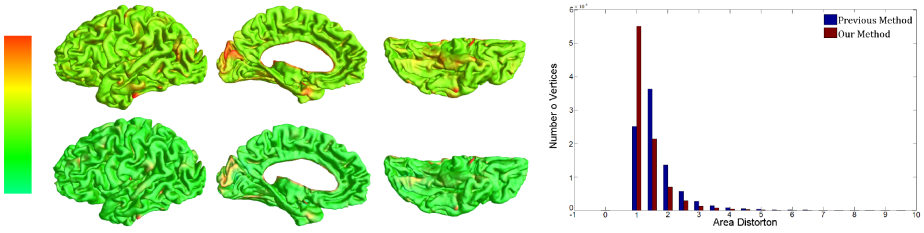

Fig. 6. Left: Average Area Distortion. Color goes from green-yellow-red while area distortion increasing. Right: Average Area Distortion of previous method and our method.

6 Conclusion and Future Work

Conventional brain mapping method suffers from the fact that with the presence of landmark constraints, the registrations may not be bijective. This work introduces a novel registration algorithm, hyperbolic harmonic mapping with curvature based landmark matching, which completely solves this problem. The new method changes the metric on Cortical surfaces and greatly improves the registration quality. Experimental results demonstrate the current method always produces smooth mapping, and outperforms some existing brain registration method in terms of curvature difference and local area distortion. In future, we will explore further the methodology of changing Riemannian metrics to improve efficiency and efficacy of different geometric algorithms.

References

1. S. Angenent, S. Haker, A. Tannenbaum, and R. Kikinis. Conformal geometry and brain flattening. In *Med. Image Comput. Comput.-Assist. Intervention*, pages 271–278, 1999.
2. M. Bakircioglu, S. Joshi, and M. I. Miller. Landmark matching on brain surfaces via large deformation diffeomorphisms on the sphere. In *Proc. SPIE Medical Imaging*, volume 3661, pages 710–715, 1999.
3. S. Durrleman, X. Pennec, A. Trouve, P. M. Thompson, and N. Ayache. Inferring brain variability from diffeomorphic deformations of currents: An integrative approach. *Medical Image Analysis*, 12(5):626–637, Oct. 2008.
4. Efrat and et al. Curve matching, time warping, and light fields: New algorithms for computing similarity between curves. *J. Math. Imaging Vis.*, 2007.
5. B. Fischl, M. I. Sereno, and A. M. Dale. Cortical surface-based analysis II: Inflation, flattening, and a surface-based coordinate system. *NeuroImage*, 9(2):195 – 207, 1999.

6. X. Gu and et al. Genus zero surface conformal mapping and its application to brain surface mapping. *IEEE Trans. Med. Imaging*, 2004.
7. A. A. Joshi and et al. A parameterization-based numerical method for isotropic and anisotropic diffusion smoothing on non-flat surfaces. *Trans. Img. Proc.*, 2009.
8. S. C. Joshi and M. I. Miller. Landmark matching via large deformation diffeomorphisms. *IEEE Trans Image Process*, 9(8):1357–1370, 2000.
9. A. Leow, C. L. Yu, S. J. Lee, S. C. Huang, R. Nicolson, K. M. Hayashi, H. Protas, A. W. Toga, and P. M. Thompson. Brain structural mapping using a novel hybrid implicit/explicit framework based on the level-set method. *NeuroImage*, 24(3):910–27, 2005.
10. D. Pantazis, A. Joshi, J. Jiang, D. W. Shattuck, L. E. Bernstein, H. Damasio, and R. M. Leahy. Comparison of landmark-based and automatic methods for cortical surface registration. *Neuroimage*, 49(3):2479–2493, Feb 2010.
11. D. Pantazis, A. A. Joshi, J. Jiang, D. W. Shattuck, L. E. Bernstein, H. Damasio, and R. M. Leahy. Comparison of landmark-based and automatic methods for cortical surface registration. *NeuroImage, Vol. 49(3), pp 2479-2493, 2009*.
12. A. Pitiot, H. Delingette, A. W. Toga, and P. M. Thompson. Learning object correspondences with the observed transport shape measure. *IPMI*, 18:25–37, 2003.
13. A. Qiu and M. I. Miller. Multi-structure network shape analysis via normal surface momentum maps. *Neuroimage*, 42(4):1430–1438, Oct 2008.
14. R. M. Schoen and S.-T. Yau. Lectures on harmonic maps. *International Press, 1997, Mathematics*.
15. D. Shen and C. Davatzikos. HAMMER: hierarchical attribute matching mechanism for elastic registration. *IEEE Trans Med Imaging*, 21(11):1421–1439, Nov 2002.
16. Y. Shi, J. H. Morra, P. M. Thompson, and A. W. Toga. Inverse-consistent surface mapping with Laplace-Beltrami eigen-features. *IPMI*, pages 467–478, 2009.
17. P. M. Thompson, J. N. Giedd, R. P. Woods, D. MacDonald, A. C. Evans, and A. W. Toga. Growth patterns in the developing human brain detected using continuum-mechanical tensor mapping. *Nature*, 404(6774):190–193, March 2000.
18. P. M. Thompson and A. W. Toga. A surface-based technique for warping 3-dimensional images of the brain. *IEEE Trans. Med. Imag.*, 15(4):1–16, 1996.
19. A. Trouvé and L. Younes. Metamorphoses through Lie group action. *Found. Comp. Math.*, pages 173–198, 2005.
20. M. Vaillant, A. Qiu, J. Glaunes, and M. I. Miller. Diffeomorphic metric surface mapping in subregion of the superior temporal gyrus. *Neuroimage*, 34(3):1149–1159, Feb 2007.
21. Y. Wang, W. Dai, X. Gu, T. F. Chan, A. W. Toga, and P. M. Thompson. Studying brain morphology using Teichmüller space theory. In *Computer Vision, 2009. ICCV 2009. IEEE 12th International Conference on*, pages 2365–2372, September 2009.
22. Y. Wang, M. Gupta, S. Zhang, S. Wang, X. Gu, D. Samaras, and P. Huang. High resolution tracking of non-rigid motion of densely sampled 3d data using harmonic maps. *Int. J. Comput. Vision*, 76(3):283–300, 2008.
23. Y. Wang, J. Shi, X. Yin, X. Gu, T. F. Chan, S. T. Yau, A. W. Toga, and P. M. Thompson. Brain surface conformal parameterization with the Ricci flow. *IEEE Trans Med Imaging*, 31(2):251–264, Feb 2012.
24. I. Yanovsky, A. D. Leow, S. Lee, S. J. Osher, and P. M. Thompson. Comparing registration methods for mapping brain change using tensor-based morphometry. *Med Image Anal*, 13(5):679–700, Oct 2009.
25. B. T. Yeo, M. R. Sabuncu, T. Vercauteren, N. Ayache, B. Fischl, and P. Golland. Spherical demons: fast diffeomorphic landmark-free surface registration. *IEEE Trans Med Imaging*, 29(3):650–668, Mar 2010.
26. W. Zeng, D. Samaras, and X. Gu. Ricci flow for 3d shape analysis. *IEEE TPAMI.*, 32:662–677, 2010.